

LEGENDRIAN AND TRANSVERSE TWIST KNOTS

JOHN B. ETNYRE, LENHARD L. NG, AND VERA VÉRTESI

ABSTRACT. In 1997, Chekanov gave the first example of a Legendrian nonsimple knot type: the $m(5_2)$ knot. Epstein, Fuchs, and Meyer extended his result by showing that there are at least n different Legendrian representatives with maximal Thurston–Bennequin number of the twist knot K_{-2n} with crossing number $2n + 1$. In this paper we give a complete classification of Legendrian and transverse representatives of twist knots. In particular, we show that K_{-2n} has exactly $\lceil \frac{n^2}{2} \rceil$ Legendrian representatives with maximal Thurston–Bennequin number, and $\lceil \frac{n}{2} \rceil$ transverse representatives with maximal self-linking number. Our techniques include convex surface theory, Legendrian ruling invariants, and Heegaard Floer homology.

1. INTRODUCTION

Throughout this paper, we consider Legendrian and transverse knots in \mathbb{R}^3 with the standard contact structure $\xi_{\text{st}} = \ker(dz - y dx)$.

A twist knot is a twisted Whitehead double of the unknot, specifically, any knot $K = K_m$ of the type shown in Figure 1. Twist knots have long been an important class of knots

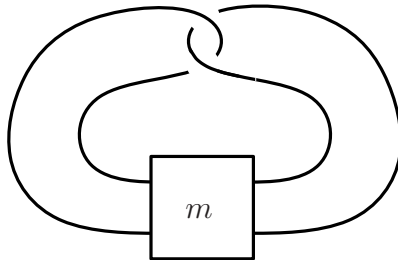


FIGURE 1. The twist knot K_m ; the box contains m right-handed half twists if $m \geq 0$, and $|m|$ left-handed half twists if $m < 0$.

to consider, particularly in contact geometry. If Legendrian knots in a given topological knot type are determined up to Legendrian isotopy by their classical invariants, namely their Thurston–Bennequin and rotation numbers, then the knot type is said to be Legendrian simple; otherwise it is Legendrian nonsimple. While there is no reason to believe all knot types should be Legendrian simple, it has historically been difficult to prove otherwise. Chekanov [2] and, independently, Eliashberg [4] developed invariants of Legendrian knots that show that $K_{-4} = m(5_2)$ has Legendrian representatives that are not determined by their classical invariants, providing the first example of a Legendrian nonsimple knot. Shortly thereafter, Epstein, Fuchs, and Meyer [6] generalized the result of Chekanov and Eliashberg to show that K_m is Legendrian nonsimple for all $m \leq -4$, and in fact that these knot types contain an

arbitrarily large number of Legendrian knots with the same classical invariants. Again these were the first such examples.

One can also ask if a knot is transversely simple, that is, are transverse knots in that knot type determined by their self-linking number? It is more difficult to prove transverse nonsimplicity than Legendrian nonsimplicity. In particular, there are knot types that are Legendrian nonsimple but transversely simple [9], whereas any transversely nonsimple knot must be Legendrian nonsimple as well. The first examples of transversely nonsimple knots were produced in 2005–6 by Birman and Menasco [1], and Etnyre and Honda [10]. It has long been suspected that some twist knots are transversely nonsimple, and this was proven very recently by Ozsváth and Stipsicz [21] using the transverse invariant in Heegaard Floer homology from [18].

Although twist knots have long supplied a useful test case for new Legendrian invariants, such as contact homology and Legendrian Heegaard Floer invariants (cf. the work of Epstein–Fuchs–Meyer and Ozsváth–Stipsicz above), a complete classification of Legendrian and transverse twist knots has been elusive. In this paper, we establish this classification and in particular identify which twist knots are Legendrian and transversely nonsimple. As a byproduct, we obtain a complete classification of an infinite family of transversely nonsimple knot types. This is one of the first (Legendrian or transversely) nonsimple families where a classification is known; see also [11].

Theorem 1.1 (Classification of Legendrian twist knots). *Let $K = K_m$ be the twist knot of Figure 1, with m half twists. We discard the case $m = -1$, which is the unknot.*

- (1) *For $m \geq -2$ even, there is a unique representative of K_m with maximal Thurston–Bennequin number, $\text{tb} = -m - 1$. This representative has rotation number $\text{rot} = 0$, and all other Legendrian knots of type K_m destabilize to the one with maximal Thurston–Bennequin number.*
- (2) *For $m \geq 1$ odd, there are exactly two representatives with maximal Thurston–Bennequin number, $\text{tb} = -m - 5$. These representatives are distinguished by their rotation numbers, $\text{rot} = \pm 1$, and a negative stabilization of the $\text{rot} = 1$ knot is isotopic to a positive stabilization of the $\text{rot} = -1$ knot. All other Legendrian knots destabilize to at least one of these two.*
- (3) *For $m \leq -3$ odd, K_m has $-\frac{m+1}{2}$ Legendrian representatives with $(\text{tb}, \text{rot}) = (-3, 0)$. All other Legendrian knots destabilize to one of these. After any positive number of stabilizations (with a fixed number of positive and negative stabilizations), these $-\frac{m+1}{2}$ representatives all become isotopic.*
- (4) *For $m \leq -2$ even with $m = -2n$, K_m has $\lceil \frac{n^2}{2} \rceil$ different Legendrian representations with $(\text{tb}, \text{rot}) = (1, 0)$. All other Legendrian knots destabilize to one of these. These Legendrian knots fall into $\lceil \frac{n}{2} \rceil$ different Legendrian isotopy classes after any given positive number of positive stabilizations, and $\lceil \frac{n}{2} \rceil$ different Legendrian isotopy classes after any given positive number of negative stabilizations. After at least one positive and one negative stabilization (with a fixed number of each), the knots all become Legendrian isotopic.*

In particular, K_m is Legendrian simple if and only if $m \geq -3$.

The content of Theorem 1.1 is depicted in the Legendrian mountain ranges in Figures 2 and 3. The Legendrian representatives of K_m with maximal Thurston–Bennequin number will be given in Section 3. Note that the cases $-3 \leq m \leq 2$ in Theorem 1.1 were already known by the classification of Legendrian unknots by Eliashberg and Fraser [5] and Legendrian torus knots and the figure eight knot by Etnyre and Honda [8].

Theorem 1.2 (Classification of transverse twist knots). *Let $K = K_m$ be the twist knot of Figure 1, with m half twists.*

- (1) *If m is even and $m \geq -2$ or m is odd, then K_m is transversely simple. Moreover, the transverse representative of K_m with maximal self-linking number has $sl = -m - 1$ if $m \geq -2$ is even, $sl = -m - 4$ if $m > -1$ is odd, $sl = -1$ if $m = -1$, and $sl = -3$ if $m < -1$ is odd.*
- (2) *If $m \leq -4$ is even with $m = -2n$, then K_m is transversely nonsimple. There are $\lfloor \frac{n}{2} \rfloor$ distinct transverse representatives of K_m with maximal self-linking number $sl = 1$. Any two of these become transversely isotopic after a single stabilization, and all other transverse representatives of K_m destabilize to one of these.*

We prove these classification theorems by using convex surface techniques, along the lines of the recipe described in [8], to produce an exhaustive list of all nondestabilizable Legendrian twist knots. This is the most technically difficult part of the proof and is deferred until Section 4. Given this list, we use the Legendrian ruling invariants of Chekanov–Pushkar and Fuchs, along with the aforementioned result of Ozsváth–Stipsicz, to distinguish nonisotopic classes of Legendrian and transverse twist knots; this is done in Section 3. We begin with a review of some necessary background in Section 2.

Acknowledgments. This paper was initiated by discussions between the last two authors at the workshop “Legendrian and transverse knots” sponsored by the American Institute of

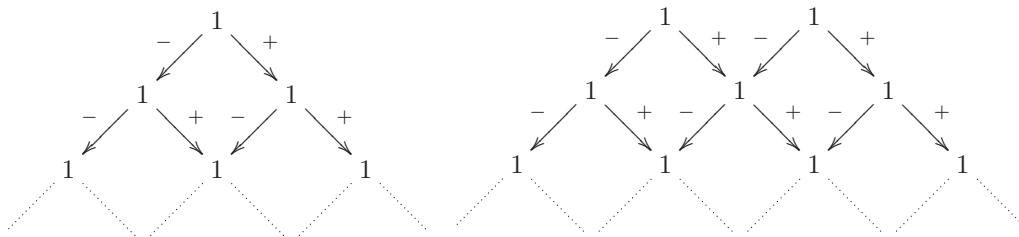


FIGURE 2. Schematic Legendrian mountain range for K_{2n} ($n \geq -1$), left, and K_{2n-1} ($n \geq 1$), right. Rotation number is plotted in the horizontal direction, Thurston–Bennequin number in the vertical direction. The numbers represent the number of Legendrian representatives for a particular (tb, rot) (here, all numbers are 1 since these knot types are Legendrian simple), and the signed arrows represent positive and negative stabilization.

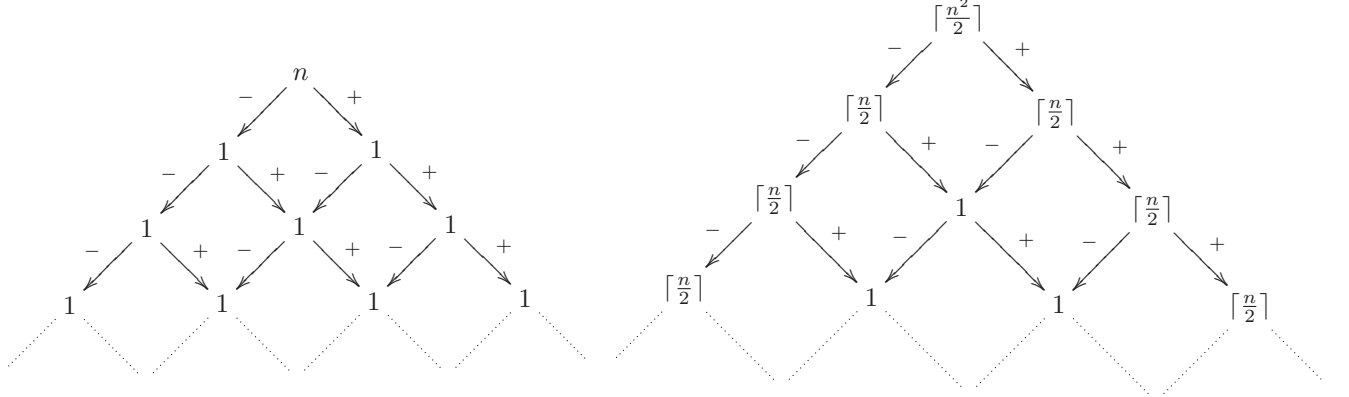


FIGURE 3. Legendrian mountain range for K_{-2n-1} ($n \geq 1$), left, and K_{-2n} ($n \geq 1$), right.

Mathematics in September 2008. We also thank Ko Honda and András Stipsicz for helpful discussions and Whitney George and the referee for valuable comments on the first draft of the paper. JBE was partially supported by NSF grant DMS-0804820. LLN was partially supported by NSF grant DMS-0706777 and NSF CAREER grant DMS-0846346. VV was partially supported by OTKA grants 49449 and 67867, and “Magyar Állami Ösztöndíj”.

2. BACKGROUND AND PRELIMINARY RESULTS

In this section we recall some basic facts about convex surfaces and bypasses, as well as ruling invariants of Legendrian knots.

2.1. Convex surfaces and bypasses. Convex surfaces are the primary tool we will use in this paper. We assume the reader is familiar with this theory at the level found in [8, 14, 15]. For the convenience of the reader and to clarify various orientation issues we will briefly recall some of the facts about convex surfaces most germane to the proofs below, but for the basic definitions and results the reader is referred to the above references.

Recall that if Σ is a convex surface and α a Legendrian arc in Σ that intersects the dividing curves Γ_Σ in 3 points p_1, p_2, p_3 (where p_1, p_3 are the endpoints of the arc), then a *bypass for Σ (along α)* is a convex disk D with Legendrian boundary such that

- (1) $D \cap \Sigma = \alpha$,
- (2) $\text{tb}(\partial D) = -1$,
- (3) $\partial D = \alpha \cup \beta$,
- (4) $\alpha \cap \beta = \{p_1, p_3\}$ are corners of D and elliptic singularities of D_ξ .

The most basic property of bypasses is how a convex surface changes when pushed across a bypass.

Theorem 2.1 (Honda [15]). *Let Σ be a convex surface and D a bypass for Σ along $\alpha \subset \Sigma$. Inside any open neighborhood of $\Sigma \cup D$ there is a (one sided) neighborhood $N = \Sigma \times [0, 1]$ of $\Sigma \cup D$ with $\Sigma = \Sigma \times \{0\}$ (if Σ is oriented, orient N so that $\Sigma = -\Sigma \times \{0\}$ as oriented manifolds) such that Γ_Σ is related to $\Gamma_{\Sigma \times \{1\}}$ as shown in Figure 4.*

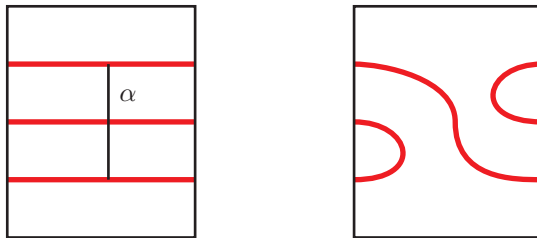


FIGURE 4. Result of a bypass attachment: original surface Σ with attaching arc α , left; the surface $\Sigma' = \Sigma \times \{1\}$, right. The dividing curves Γ_Σ and $\Gamma_{\Sigma'}$ are shown as thicker curves.

In the above discussion the bypass is said to be attached from the front. To attach a bypass from the back one needs to change the orientation of the interval $[0, 1]$ in the above theorem and mirror Figure 4.

If Σ and Σ' are two convex surfaces, $\partial\Sigma'$ is a Legendrian curve contained in Σ , and $\Sigma \cap \Sigma' = \partial\Sigma'$, then if Σ' has a boundary parallel dividing curve (and there are other dividing curves on Σ') then one can always find a bypass for Σ contained in Σ' (and containing the boundary parallel dividing curve). This is a simple application of the Legendrian realization principle [17]. It is useful to be able to find bypasses in other ways too. For this we have the notion of bypass rotation.

Lemma 2.2 (Honda, Kazez, and Matic [16]). *Suppose Σ is a convex surface containing a disk D such that $D \cap \Gamma_\Sigma$ is as shown in Figure 5. Also suppose δ and δ' are as shown in the figure. If there is a bypass for Σ attached along δ from the front side of the diagram, then there is a bypass for Σ attached along δ' from the front.*

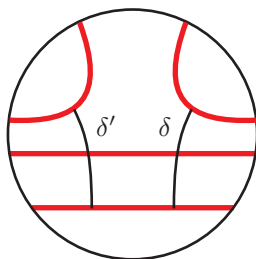


FIGURE 5. If there is a bypass for δ then there is one for δ' as well.

We end our brief review of convex surfaces by describing how two convex surfaces that come together along a Legendrian circle in their boundary can be made into a single convex surface by rounding their corners.

Lemma 2.3 (Honda [15]). *Suppose that Σ and Σ' are convex surfaces with dividing curves Γ and Γ' respectively, and $\partial\Sigma' = \partial\Sigma$ is Legendrian. Model Σ and Σ' in \mathbb{R}^3 by $\Sigma = \{(x, y, z) : x = 0, y \geq 0\}$ and $\Sigma' = \{(x, y, z) : y = 0, x \geq 0\}$. Then we may form a surface Σ'' from $S = \Sigma \cup \Sigma'$ by replacing S in a small neighborhood N of $\partial\Sigma$ (thought of as the z -axis) with the intersection of N with $\{(x, y, z) : (x - \delta)^2 + (y - \delta)^2 = \delta^2\}$. For a suitably chosen δ , Σ'' will be a smooth surface (actually just C^1 , but it can then be smoothed by a C^1 small isotopy which can easily be seen not to change the characteristic foliation) with dividing curve as shown in Figure 6.*

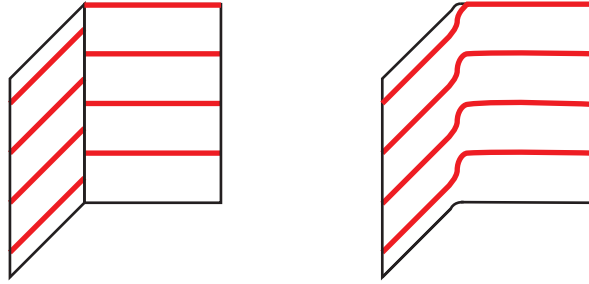


FIGURE 6. Rounding a corner between two convex surfaces. On the left, $\Sigma \cup \Sigma'$; on the right, Σ'' .

In this lemma, rounding a corner causes the dividing curves on the two surfaces to connect up as follows: moving from Σ to Σ' , the dividing curves move up (down) if Σ' is to the right (left) of Σ .

2.2. Ruling invariants. In order to distinguish between Legendrian isotopy classes of twist knots in Section 3, we use invariants of Legendrian knots in standard contact \mathbb{R}^3 known as the ρ -graded ruling invariants, as introduced by Chekanov–Pushkar [22] and Fuchs [13]. Here we very briefly recall the relevant definitions and results; for further details, see, e.g., the above papers or [7].

Given the front (xz) projection of a Legendrian knot in \mathbb{R}^3 , a *ruling* is a one-to-one correspondence between left and right cusps, along with a decomposition of the front as a union of pairs of paths beginning at a left cusp and ending at the corresponding right cusp, satisfying the following conditions:

- all paths are smooth except possibly at double points (crossings) in the front, and never change direction with respect to x coordinate;
- the two paths for a particular pair of cusps do not intersect except at the two cusp endpoints;
- any two arbitrary paths intersect at most at cusps and crossings;

- at a crossing where two paths (which must necessarily have different endpoints) intersect and one lies entirely above the other (such a crossing is a *switch*), the two paths and their companion paths must be arranged locally as in Figure 7.

See Figure 8 for examples of rulings; note that a ruling is uniquely determined by its switches, and can be thought of as a “partial 0-resolution” of the front.

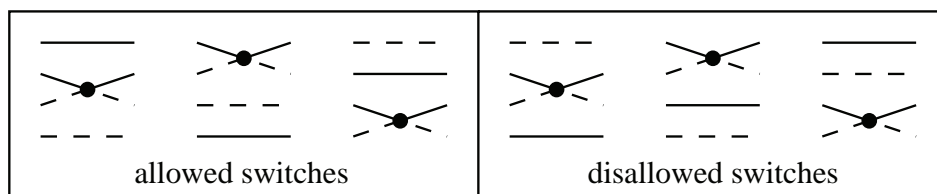


FIGURE 7. Allowed and disallowed switches in a ruling. In each diagram, the two solid arcs are paired together (i.e., share cusp endpoints), as are the two dashed arcs. Other pairs of arcs, which may be present, are not shown.

One can refine the concept of a ruling by considering Maslov degrees. Removing the $2c$ left and right cusps from a front (not necessarily with a ruling) yields $2c$ arcs, each connecting a left cusp to a right cusp. If rot is the rotation number of the front, then we can assign integers (*Maslov numbers*) mod 2rot to each of these arcs so that at each cusp, the upper arc (with higher z coordinate) has Maslov number 1 greater than the lower arc; for a connected front, these numbers are well-defined up to adding a constant to all arcs. To each crossing in the front, we can define the *Maslov degree* to be the Maslov number of the strand with more negative slope minus the Maslov number of the strand with more positive slope. Finally, if ρ is any integer dividing 2rot , then we say that a ruling of the front is ρ -graded if all switches have Maslov degree divisible by ρ . In particular, a 1-graded ruling (also known as an ungraded ruling) is a ruling with no condition on the switches.

Proposition 2.4 (Chekanov and Pushkar [22]). *Let \mathcal{K} be a Legendrian knot with rotation number $\text{rot}(\mathcal{K})$. For any ρ dividing $2\text{rot}(\mathcal{K})$, the number of ρ -graded rulings of the front of \mathcal{K} is an invariant of the Legendrian isotopy class of \mathcal{K} .*

The existence of rulings is closely related to the maximal Thurston–Bennequin number of a knot.

Proposition 2.5 (Rutherford [23]). *If a Legendrian knot \mathcal{K} admits an ungraded ruling, then it maximizes Thurston–Bennequin number within its topological class.*

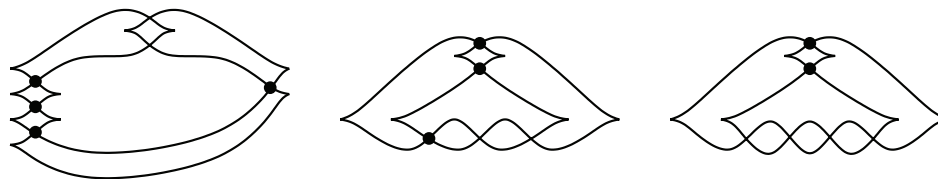


FIGURE 8. Rulings of Legendrian versions of the twist knots K_{-4} , K_3 , and K_4 . Dots indicate switches.

For twist knots, Proposition 2.5 allows easy calculation of the maximal value of tb ; we note that the following result can also be derived from the more general calculation for two-bridge knots from [19].

Proposition 2.6. *The maximal Thurston–Bennequin number for K_m is:*

$$\overline{\text{tb}}(K_m) = \begin{cases} -m - 1 & m \geq 0 \text{ even} \\ -m - 5 & m \geq 1 \text{ odd} \\ -1 & m = -1 \\ 1 & m \leq -2 \text{ even} \\ -3 & m \leq -3 \text{ odd.} \end{cases}$$

Proof. Figure 8 shows ungraded rulings for Legendrian forms of K_{-4} , K_3 , and K_4 ; these have obvious generalizations to Legendrian knots of type K_m for $m \leq -2$, $m \geq 1$ odd, and $m \geq 0$ even, respectively, each of which has an ungraded ruling. It follows from Proposition 2.5 that each of these knots maximizes tb . Easy calculations of Thurston–Bennequin numbers for each case (along with the fact that K_{-1} is the unknot) yield the proposition. \square

3. THE CLASSIFICATION OF LEGENDRIAN TWIST KNOTS

In this section we will classify Legendrian and transverse twist knots by proving Theorems 1.1 and 1.2. We begin with several preliminary results that will be proved in Section 4.

Theorem 3.1. *For $m \leq -2$, any Legendrian representative of $K = K_m$ with maximal tb is Legendrian isotopic to some Legendrian knot whose front projection is of the form depicted in Figure 9, where the rectangle contains $|m + 2|$ negative half twists each of which is of type Z or S .*

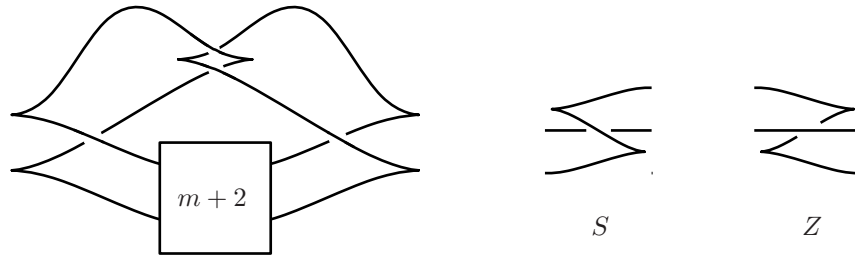


FIGURE 9. A front projection for K_m for $m \leq -2$, and half twists of type S and Z .

Theorem 3.2. *For $m \geq 0$, any Legendrian representative of $K = K_m$ with maximal tb is Legendrian isotopic to the Legendrian knot with front projection depicted in Figure 10, where the rectangle contains m positive half twists each of which is of type X .*

The techniques developed for the proof of the above theorems also give the following result.

Theorem 3.3. *Let \mathcal{K} be a Legendrian representative of the twist knot K_m . Whenever $\text{tb}(\mathcal{K}) < \overline{\text{tb}}(K_m)$ then \mathcal{K} destabilizes.*

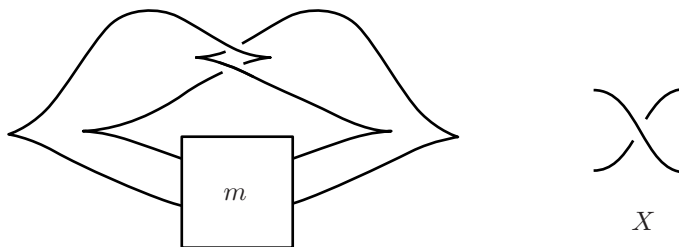


FIGURE 10. A front projection for K_m for $m \geq 0$, and crossings of type X .

We will see below that Theorems 3.2 and 3.3 establish Items (1) and (2) in Theorem 1.1, the classification of Legendrian K_m for $m \geq -2$. To classify Legendrian K_m for $m \leq -3$, we need to distinguish between the distinct representatives of K_m with maximal Thurston–Bennequin number and understand when they become the same under stabilization.

We begin by considering K_m when $m \leq -4$ is even. According to Theorem 3.1, we can represent each of the maximal-tb representatives of K_{-2n} by a length $2n - 2$ word in the letters Z^+, Z^-, S^+, S^- , where these letters represent the Legendrian half-twists shown in Figure 11 and letters must alternate in sign. Given such a word w , let $z^+(w), z^-(w), s^+(w), s^-(w)$ denote the number of Z^+, Z^-, S^+, S^- in w , respectively, and note that $z^+(w) + s^+(w) = z^-(w) + s^-(w) = n - 1$.

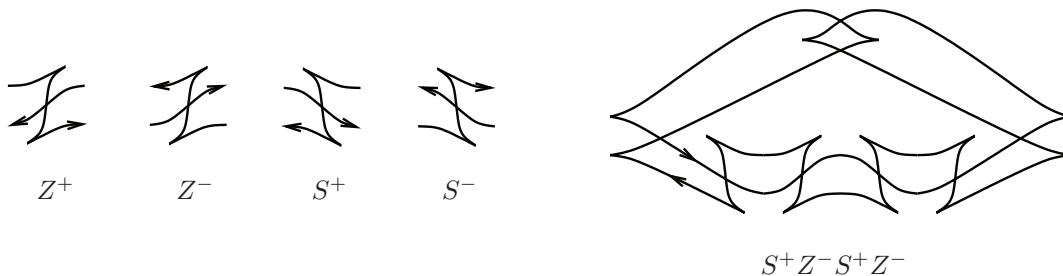
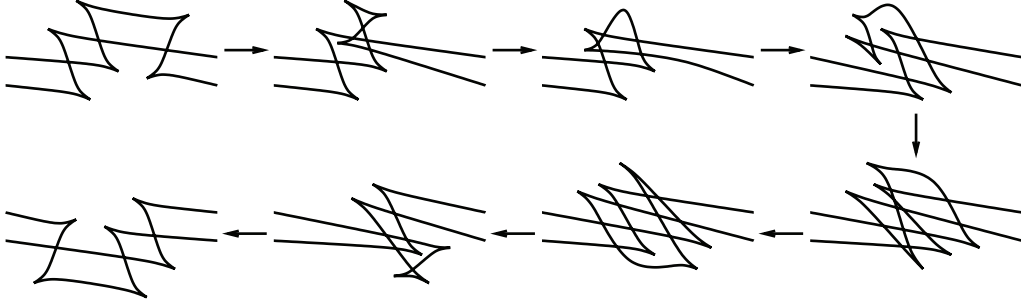
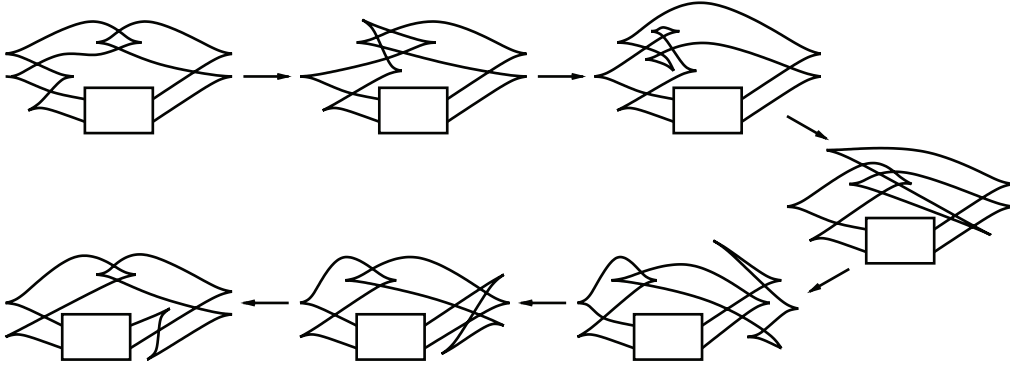


FIGURE 11. Denoting a maximal-tb twist knot by a word in Z 's and S 's.

Lemma 3.4. *Two words of length $2n$ with the same z^+, z^-, s^+, s^- correspond to Legendrian-isotopic knots.*

Proof. A local computation (Figure 12) shows that $S^\pm S^\mp Z^\pm$ and $Z^\pm S^\mp S^\pm$ are Legendrian isotopic as Legendrian tangles. (Alternately, the fact that these are Legendrian isotopic follows from the Legendrian satellite construction [20].) Similarly, $Z^\pm Z^\mp S^\pm$ and $S^\pm Z^\mp Z^\pm$ are Legendrian isotopic. It follows that we can transpose consecutive $+$ letters in a word while preserving Legendrian-isotopy class, and the same for consecutive $-$ letters. Thus two words with the same z^+, z^-, s^+, s^- that begin with the same sign correspond to Legendrian-isotopic knots.

FIGURE 12. Legendrian isotopy between SSZ and ZSS .FIGURE 13. Moving a Z from the beginning of a word to the end.

To complete the proof, it suffices to show that $Z^\pm w$ and wZ^\pm correspond to Legendrian isotopic knots for a length $2n - 3$ word w , as do $S^\pm w$ and wS^\pm . For $Z^\pm w = wZ^\pm$, see Figure 13; for $S^\pm w = wS^\pm$, reflect Figure 13 in the vertical axis. \square

By Lemma 3.4, we can define Legendrian isotopy classes \mathcal{K}_{z^+, z^-} for $0 \leq z^\pm \leq n - 1$ corresponding to words with the specified z^+, z^- . We then have the following result.

Lemma 3.5. *The Legendrian isotopy classes \mathcal{K}_{z^+, z^-} and $\mathcal{K}_{n-1-z^+, n-1-z^-}$ are the same.*

Proof. The map $(x, y, z) \mapsto (-x, -y, z)$ is a contactomorphism of \mathbb{R}^3 that preserves Legendrian isotopy classes, as can easily be seen in the xy projection, where it is a rotation by 180° . In the xz projection, this map sends tangles Z^\pm to S^\pm and S^\pm to Z^\pm and thus sends \mathcal{K}_{z^+, z^-} to $\mathcal{K}_{n-1-z^+, n-1-z^-}$. \square

We are now in a position to classify the \mathcal{K}_{z^+, z^-} 's and all Legendrian knots obtained from the \mathcal{K}_{z^+, z^-} 's by stabilization. The key ingredients are a result of Ozsváth and Stipsicz [21] on distinct transverse representatives of twist knots, and the ruling invariant discussed in Section 2.2. Let St^+, St^- denote the operations on Legendrian isotopy classes given by positive and negative stabilization.

Proposition 3.6. *For $0 \leq z^\pm, z^{\pm'} \leq n - 1$, we have:*

- (1) \mathcal{K}_{z^+, z^-} is Legendrian isotopic to \mathcal{K}_{z^+, z^-} if and only if $(z^+, z^-) = (z^+, z^-)$ or $(z^+, z^-) = (n-1-z^+, n-1-z^-)$;
- (2) \mathcal{K}_{z^+, z^-} and \mathcal{K}_{z^+, z^-} are Legendrian isotopic after some positive number of positive stabilizations if and only if $z^- = z^-$ or $z^- = n-1-z^-$, and in these cases the knots are isotopic after one positive stabilization;
- (3) \mathcal{K}_{z^+, z^-} and \mathcal{K}_{z^+, z^-} are Legendrian isotopic after some positive number of negative stabilizations if and only if $z^+ = z^+$ or $z^+ = n-1-z^+$, and in these cases the knots are isotopic after one negative stabilization;
- (4) $St^+ St^- \mathcal{K}_{z^+, z^-}$ is Legendrian isotopic to $St^+ St^- \mathcal{K}_{z^+, z^-}$ for all $z^\pm, z^{\pm'}$.

Proof. We first establish (3). It is well-known [6] that Z^- and S^- become Legendrian isotopic after one negative stabilization; see Figure 14. Consequently, for $z^- < n-1$, $St^- \mathcal{K}_{z^+, z^-} = St^- \mathcal{K}_{z^+, z^-+1}$, and thus $St^- \mathcal{K}_{z^+, z^-} = St^- \mathcal{K}_{z^+, z^-} = St^- \mathcal{K}_{n-1-z^+, z^-}$ for any z^+, z^-, z^-, z^- , where the last equality follows from Lemma 3.5. On the other hand, by [21], if $0 \leq z^+, z^+ \leq n/2$ with $z^+ \neq z^+$, then \mathcal{K}_{z^+, z^+} and \mathcal{K}_{z^+, z^+} represent distinct Legendrian isotopy classes even after any number of negative stabilizations. (Note that \mathcal{K}_{z^+, z^+} can be represented by the word $(Z^- Z^+)^{z^+} (S^- S^+)^{n-1-z^+}$, which corresponds to the Legendrian knot $E(2z^+ + 1, 2n - 2z^+ - 1)$ in the notation of [21].)

Item (3) follows, and (2) is proved similarly. Item (4) is an immediate consequence of (2) and (3), since stabilizations commute: $St^+ St^- \mathcal{K}_{z^+, z^-} = St^+ St^- \mathcal{K}_{z^+, z^-} = St^- St^+ \mathcal{K}_{z^+, z^-} = St^+ St^- \mathcal{K}_{z^+, z^-}$.

It remains to establish (1). The “if” part follows from Lemma 3.5. For “only if”, we use graded ruling invariants; one could also use Legendrian contact homology [2]. The Maslov



FIGURE 14. Z and S tangles are isotopic after an appropriate stabilization of each.

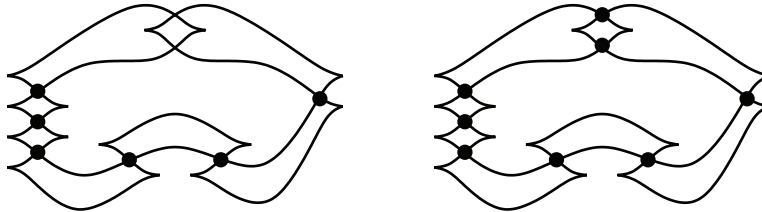


FIGURE 15. All possible ρ -graded rulings of the front for \mathcal{K}_{z^+, z^-} (pictured here, $ZZSZ$ with either orientation). Dots indicate switches. The left ruling is ρ -graded for any ρ ; all switches have Maslov degree 0. The two new switches in the right ruling have Maslov degree $2(z^+ + z^- + 1 - n)$ (top) and $-2(z^+ + z^- + 1 - n)$ (bottom), and thus the right ruling is ρ -graded if and only if ρ divides $2(z^+ + z^- + 1 - n)$.

degrees of the two uppermost (clasp) crossings in a representative front diagram for \mathcal{K}_{z^+, z^-} are readily seen to be $\pm 2(z^+ + z^- + 1 - n)$. It follows from this that there is exactly one ρ -graded (normal) ruling of the front unless $\rho \mid 2(z^+ + z^- + 1 - n)$, in which case there are two ρ -graded rulings; See Figure 15.

Now suppose that $\mathcal{K}_{z^+, z^-} = \mathcal{K}_{z^{+'}, z^{-'}}$. By Proposition 2.4, we must have $|z^+ + z^- + 1 - n| = |z^{+'} + z^{-'} + 1 - n|$. On the other hand, by (2) and (3), $z^{+'} \in \{z^+, n - 1 - z^+\}$ and $z^{-'} \in \{z^-, n - 1 - z^-\}$. Combined, these equations imply that $(z^{+'}, z^{-'}) = (z^+, z^-)$ or $(n - 1 - z^+, n - 1 - z^-)$, as desired. \square

We next consider K_m when $m \leq -3$ is odd, say $m = -2n - 1$; the argument here is similar to, but simpler than, the case of $m \leq -4$ even. According to Theorem 3.1, we can represent each of the maximal-tb representatives of K_{-2n-1} by a length $2n - 1$ word in the letters Z^+, Z^-, S^+, S^- , where these letters represent the Legendrian half-twists shown in Figure 11 and letters must alternate in sign and begin and end with the same sign. The Legendrian isotopy at the end of the proof of Lemma 3.4 shows that we may assume that the word begins (and ends) with a letter with a plus sign. As above, given such a word w , let $z^+(w), z^-(w), s^+(w), s^-(w)$ denote the number of Z^+, Z^-, S^+, S^- in w , respectively, and note that $z^+(w) + s^+(w) = z^-(w) + s^-(w) + 1 = n$.

Essentially the same proof as for Lemma 3.4 gives the following result.

Lemma 3.7. *Two words of length $2n-1$ with the same z^+, z^-, s^+, s^- correspond to Legendrian-isotopic knots.* \square

By Lemma 3.7, we can define Legendrian isotopy classes \mathcal{K}_{z^+, z^-} for $0 \leq z^\pm \leq n$ corresponding to words with the specified z^+, z^- . We then have the following result.

Lemma 3.8. *The Legendrian isotopy classes \mathcal{K}_{z^+, z^-} and $\mathcal{K}_{n-z^+, n-1-z^-}$ are the same. If $z^+ < n$ and $z^- \geq 1$, then the Legendrian isotopy classes of \mathcal{K}_{z^+, z^-} and $\mathcal{K}_{z^++1, z^- - 1}$ are the same.*

Proof. The first statement follows as in the proof of Lemma 3.5. For the second statement, let S^+Z^-w' be a word representing \mathcal{K}_{z^+, z^-} , where w' is some word of length $2n - 3$; then Z^+S^-w' represents $\mathcal{K}_{z^++1, z^- - 1}$. The isotopy in Figure 13 shows that Z^+S^-w' and $S^-w'Z^-$ correspond to Legendrian isotopic knots, while the reflection of this isotopy in the z axis shows that S^+Z^-w' and $Z^-w'S^-$ correspond to Legendrian isotopic knots. But $S^-w'Z^-$ and $Z^-w'S^-$ are also Legendrian isotopic by Lemma 3.7. \square

It follows from Theorem 3.1 and Lemma 3.8 that every maximal-tb knot has a representative of the form \mathcal{K}_{n, z^-} for some $0 \leq z^- \leq n - 1$; we denote this representative by \mathcal{K}_{z^-} .

Proposition 3.9. *For $0 \leq z^-, z^{-'} \leq n - 1$, we have:*

- (1) \mathcal{K}_{z^-} is Legendrian isotopic to $\mathcal{K}_{z^{-'}}$ if and only if $z^{-'} = z^-$;
- (2) $St^\pm \mathcal{K}_{z^-}$ is Legendrian isotopic to $St^\pm \mathcal{K}_{z^{-'}}$ for all $z^-, z^{-'}$.

Proof. The proof of (2) is exactly the same as the proof of (2) and (3) in Proposition 3.6. For Item (1) we again use ρ -graded rulings. As in the proof of Proposition 3.6, all of the crossings in \mathcal{K}_{z^-} have Maslov degree 0, except for the top two crossings, which have grading $\pm(2z^- + 1)$.

So K_{z^-} has one ρ -graded ruling unless $2z^- + 1$ is divisible by ρ , in which case it has two. By Proposition 2.4, \mathcal{K}_{z^-} and $\mathcal{K}_{z^{-\prime}}$ cannot be Legendrian isotopic unless $z^- = z^{-\prime}$. \square

We are now ready for the proof of our main theorem.

Proof of Theorem 1.1. We begin with Items (1) and (2) of the theorem concerning the knot type K_m with $m \geq 0$ (the case $m = -2$ is covered by (4)). Theorem 3.2 says that there is a unique Legendrian representative for K_m with maximal Thurston–Bennequin number if orientations are ignored. For m odd, when we take orientations into account, there are two maximal tb representatives \mathcal{K}_+ and \mathcal{K}_- of K_m and they are distinguished by their rotation numbers, $\text{rot}(\mathcal{K}_{\pm}) = \pm 1$. Using the isotopy described in the proof of Lemma 3.5, one easily verifies that $St^-(\mathcal{K}_+)$ is Legendrian isotopic to $St^+(\mathcal{K}_-)$. Since Theorem 3.3 says that all other representatives destabilize to \mathcal{K}_{\pm} , we conclude that K_m is Legendrian simple if $m \geq 1$ is odd. When $m \geq 0$ is even, one may again use the isotopy described in the proof of Lemma 3.5 to check that the two oriented Legendrian representatives of K_m coming from Theorem 3.2 are Legendrian isotopic. Thus there is a unique representative of K_m with maximal Thurston–Bennequin number and all other Legendrian representatives are stabilizations of this one. This completes the proof for $m \geq 0$.

Next consider the case when m is negative and even. The maximal Thurston–Bennequin number representatives of K_{-2n} are of the form \mathcal{K}_{z^+, z^-} for $z^+, z^- \in \{0, \dots, n-1\}$, by Theorem 3.1. (This is even true after considering possible orientations, since the orientation reverse of \mathcal{K}_{z^+, z^-} is \mathcal{K}_{z^-, z^+} .) Moreover, Proposition 3.6 says $\mathcal{K}_{z^+, z^-} = \mathcal{K}_{z^{+\prime}, z^{-\prime}}$ if and only if $(z^{+\prime}, z^{-\prime}) = (z^+, z^-)$ or $(z^{+\prime}, z^{-\prime}) = (n-1-z^+, n-1-z^-)$. Since there are n choices for z^+ and z^- it is clear that there are $\lceil \frac{n^2}{2} \rceil$ distinct representatives. Similarly we see that after strictly positive or strictly negative stabilizations there are $\lceil \frac{n}{2} \rceil$ distinct representatives and after both type of stabilizations there is just one representative. This completes the proof of Item (4) of the theorem.

Similarly, when $m = -2n - 1$ is negative and odd, Item (1) in Proposition 3.9 implies there are at least n Legendrian representatives with maximal tb, while Lemma 3.8 and the discussion around it implies there are at most n . Moreover Theorem 3.3 says all Legendrian representatives with non-maximal tb destabilize to one of these. Thus Item (3) of the theorem is completed by Item (2) in Proposition 3.9. \square

Proof of Theorem 1.2. We use the fact, due in this setting to [6], that the negative stable classification of Legendrian knots is equivalent to the classification of transverse knots. More precisely, two transverse knots are transversely isotopic if and only if any of their Legendrian approximations are Legendrian isotopic after some number of negative stabilizations. Then Theorem 1.2 is a direct corollary of Theorem 1.1. \square

4. NORMALIZING THE FRONT PROJECTION

In this section we prove Theorems 3.1, 3.2, and 3.3, thus completing the proof of our main Theorem 1.1. To this end, notice that since K_m is a rational knot, we can find an embedded 2-sphere S in $S^3 (= \mathbb{R}^3 \cup \{\infty\})$ intersecting K_m in four points and dividing K_m into unknotted pieces. More precisely, we can choose S as shown in Figure 16, intersecting K in four points labeled 1, 2, 3 and 4 in the figure and separating S^3 into two balls B_{in} and

B_{out} , such that: K_m intersects B_{out} as a (vertical) 2-braid with two negative half-twists, which we denote $K_{\text{out}} = K \cap B_{\text{out}}$, and K_m intersects B_{in} as a (horizontal) 2-braid with m positive half-twists, which we denote $K_{\text{in}} = K \cap B_{\text{in}}$.

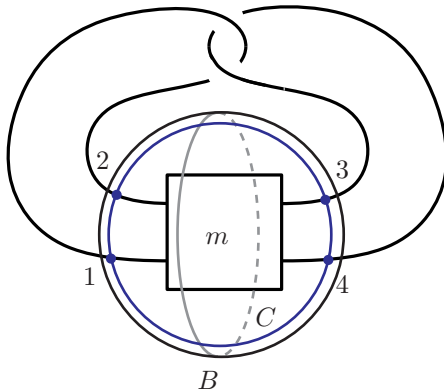


FIGURE 16. Model of the knot K_m , intersecting a 2-sphere S in four points. The closed curve C on S intersects K_m in four points and the closed curve B on S separates the points 1, 2 from 3, 4.

We begin by normalizing the dividing curves on S . After this we study the contact structures on the 3-balls B_{in} and B_{out} .

4.1. Normalizing the sphere S . Throughout this section, we fix a standard model for K_m as shown in Figure 16, and we assume $m \neq -1$. A Legendrian realization \mathcal{K} of K_m defines an isotopy $\psi: S^3 \rightarrow S^3$ mapping K_m to \mathcal{K} and S to $\psi(S)$. We can change the isotopy ψ such that $\psi(S)$ is a convex surface, and a standard neighborhood N of \mathcal{K} with meridional ruling curves intersects $\psi(S)$ in four Legendrian unknots. Let P be the sphere with four punctures $P = S \setminus \nu(K_m)$. The position of the pullback Γ_P of the dividing curves on $\psi(P)$ depends on the chosen convex representation of $\psi(S)$, and thus on the isotopy ψ , but we can always choose ψ so that Γ_P is normalized as follows.

Theorem 4.1. *Let $m \neq -1$, and fix K_m along with a neighborhood $\nu(K_m)$ and the surfaces S and P as above. For any Legendrian realization \mathcal{K} of K_m , there exists an isotopy $\psi: S^3 \rightarrow S^3$ such that S (and thus P) is convex, $\psi(\nu(K_m)) = N$ is a standard contact neighborhood of \mathcal{K} , and the pullback $\Gamma_P \subset P$ of the dividing curves on $\psi(P)$ is as shown in Figure 17.*

Before proving Theorem 4.1, we establish the following lemma.

Lemma 4.2. *If $m \neq -1$ and \mathcal{K} is a Legendrian realization of K_m , then there is a Legendrian unknot \mathcal{L} with $\text{tb}(\mathcal{L}) = -1$ that, in the complement of \mathcal{K} , is topologically isotopic to the curve B in Figure 16.*

Proof. There exists some Legendrian knot \mathcal{L} in the topological class of B , disjoint from K_m . Suppose that \mathcal{L} has been chosen so that $\text{tb}(\mathcal{L})$ is maximal for Legendrians in this class, say $\text{tb}(\mathcal{L}) = -n$ for some $n > 0$. We will show that the assumption that $n > 1$ leads to a contradiction.

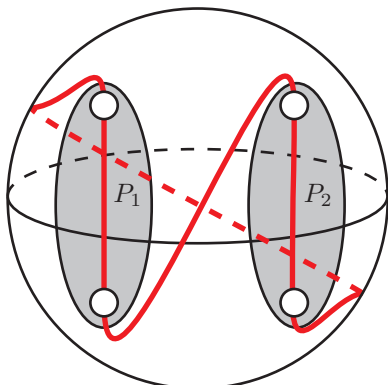


FIGURE 17. The dividing curves on P can always be arranged to be as shown (assuming $m \neq -1$).

Let $N_{\mathcal{L}}$ be a standard neighborhood of \mathcal{L} disjoint from \mathcal{K} . Set $Q = \overline{(S^3 - N_{\mathcal{L}})}$. Clearly Q is a solid torus $S^1 \times D^2$ with convex boundary, and the boundary has two dividing curves of slope $-n$. We can assume the ruling curves are meridional and then choose two disks D_1 and D_2 in Q bounding these ruling curves as shown in Figure 18. Specifically, $\partial Q \setminus (\partial D_1 \cup \partial D_2)$

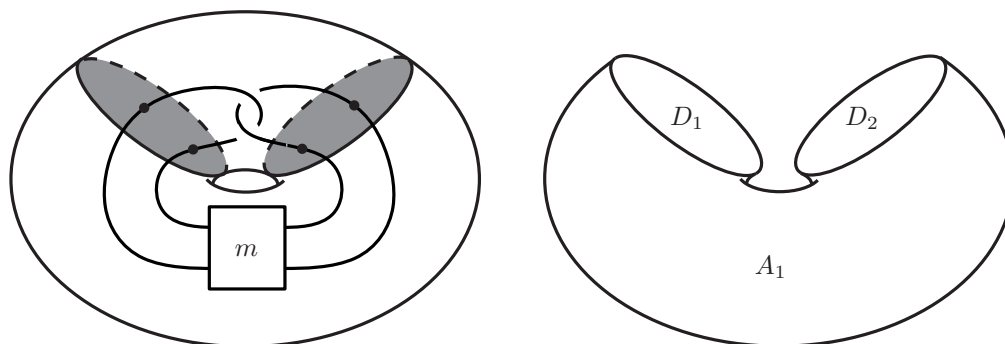


FIGURE 18. The torus $\partial Q = \partial N_L$ on the left with the disk D_1 and D_2 shaded. On the right is the annulus A_1 and the disks D_1 and D_2 whose union can be taken to be S .

consists of two annuli A_1 and A_2 such that $A_1 \cup D_1 \cup D_2$ (after rounding corners) represents the sphere S . We can isotop each D_i so that a standard neighborhood N of \mathcal{K} intersects D_i in two disks with Legendrian boundary (which are meridional ruling curves on ∂N) and D_i is convex. Let $P_i = D_i \setminus N$. Then P_i is a pair of pants with three boundary components, which we label $c_{i,1}, c_{i,2}, c_{i,3}$ such that $c_{i,3}$ is the boundary component contained in ∂Q and $c_{i,1}, c_{i,2}$ are ruling curves in ∂N .

Notice that $\Gamma_{P_i} = \Gamma_P \cap P_i$ intersects each of $c_{i,1}$ and $c_{i,2}$ exactly twice and intersects $c_{i,3}$ exactly $2n$ times. If Γ_{D_i} has more than two boundary parallel dividing curves then Γ_{P_i} will have at least one boundary parallel dividing curve along $c_{i,3}$ and thus we can use this to construct a bypass to destabilize \mathcal{L} in the complement of \mathcal{K} . As this is a contradiction, we

know the dividing curves on P_i can be described in the following way; see Figure 19 for an illustration. There is a coordinate system on D_i so that:

- D_i is the unit disk in the xy plane;
- $\mathcal{K} \cap D_i$ is $\{(0, \pm 1/2)\}$;
- $C \cap D_i$ is the line segment $x = 0$, where C is as shown in Figure 16;
- P_i is D_i with small disks around $(0, \pm 1/2)$ removed.

Let $A_{i,j}$ be small annular neighborhoods of $c_{i,j}$ in P_i , and let P'_i be the closure of the complement of these annuli in P_i . For $n > 1$, the dividing curves on P'_i can be assumed to be $n - 2$ horizontal line segments, along with the line segments in P'_i given by $y = \pm 1/2$. In addition, in each $A_{i,j}$, the dividing curves can be assumed to be the obvious extension of the dividing curves in P'_i , with some number of half-twists in $A_{i,1}$ and $A_{i,2}$ and some rigid rotation in $A_{i,3}$. To elaborate on this last point, identify the closure of $A_{i,3}$ radially with $S^1 \times [0, 1]$ so that $\Gamma_{P_i} \cap (S^1 \times \{0\})$ is $2n$ equally spaced points p_1, \dots, p_{2n} in the circle $c_{i,3}$ and $\Gamma_{P_i} \cap (S^1 \times \{1\})$ is the corresponding set of $2n$ points p'_1, \dots, p'_{2n} in the other boundary component of $A_{i,3}$; then in $A_{i,3}$, Γ_{P_i} consists of $2n$ nonintersecting segments connecting p_1, \dots, p_{2n} to p'_1, \dots, p'_{2n} in some (cyclically permuted) order.

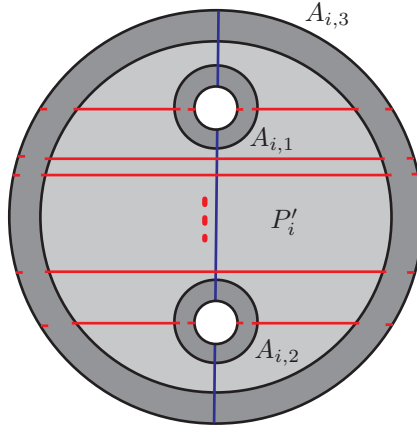


FIGURE 19. The disk D_i . The lightly shaded region is P'_i and the darkly shaded regions are the annuli $A_{i,j}$; the union of all the shaded regions is P_i ; the vertical line is $C \cap P_i$; and the horizontal lines are the dividing curves Γ_{P_i} . In the darkly shaded regions, the dividing curves cross from one boundary component to the other.

After rounding the corners of $D_1 \cup D_2 \cup A_1$, define A to be the annulus $A_1 \cup A_{1,3} \cup A_{2,3}$. Notice that on A there are $2n$ dividing curves running from one boundary component to the other (we know the dividing curves on A_1 as A_1 is part of $\partial N_{\mathcal{L}} = \partial Q$); let Γ_A denote the union of these dividing curves. As above we can choose a product structure $S^1 \times [0, 1]$ on the closure of A so that S^1 has length $2n$, $\Gamma_A \cap (S^1 \times \{0\})$ and $\Gamma_A \cap (S^1 \times \{1\})$ each consists of $2n$ equally spaced points, and Γ_A connects these two sets of points through $2n$ nonintersecting segments. The dividing curve on the 2-sphere S must be connected since we are in a tight contact structure, and thus the slope s of the curves in Γ_A must be relatively prime to n .

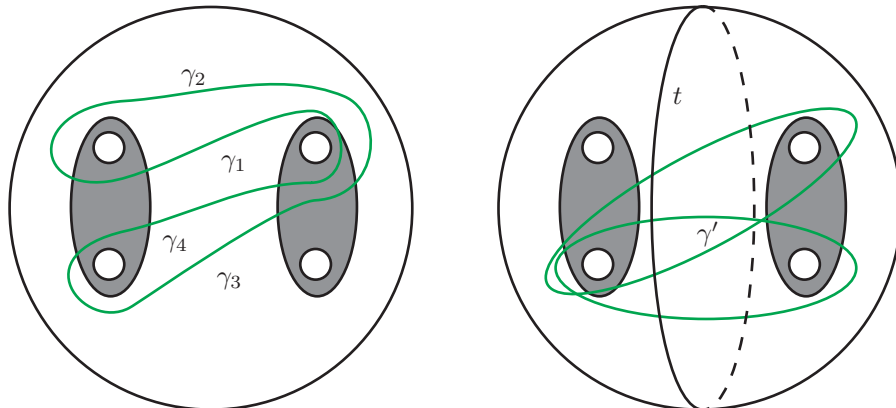


FIGURE 20. The sphere S with P'_1 and P'_2 shaded. The curve γ is shown on the left and its intersection with the white annulus A consists of the four curves $\gamma_1, \gamma_2, \gamma_3, \gamma_4$. If m is even then γ' is the image of the horizontal curve on the right after $\frac{m}{2}$ Dehn twists along the curve t and if m is odd then it is the image of the diagonal curve on the right after $\frac{m-1}{2}$ Dehn twists along the curve t .

Define curves γ and γ' in S as shown in Figure 20. Then γ and γ' bound disks D_{out} in B_{out} and D_{in} in B_{in} , respectively, where both disks are disjoint from \mathcal{K} . We can assume that both γ and γ' intersect the dividing curves of S only in A , and that the curve γ intersects A in four arcs $\gamma_1, \gamma_2, \gamma_3, \gamma_4$ as shown in Figure 20. If γ is isotoped so that it intersects the P'_i in horizontal arcs, then using the above identification of the closure of A with $S^1 \times [0, 1]$, the slopes of γ_i can be taken to be $2, 0, n, n - 2$, respectively. Similarly γ' intersects A in two parallel linear arcs γ'_1 and γ'_2 of slope nm .

Legendrian realize γ and γ' , and make D_{out} and D_{in} convex. If γ or γ' does not have maximal tb , then D_{out} or D_{in} has at least two boundary-parallel dividing curves and thus there are at least two bypasses for $S \setminus N_{\mathcal{L}}$ in the complement of \mathcal{K} . (Notice that when there are only two dividing curves the two bypasses are not disjoint, however we will see below that we will only need one bypass in this case, and in most cases.) Let c be the curve along which one of the bypasses is attached. (Note that since γ' bounds a disc in B_{in} the bypass in that case is attached from the back so its action on the dividing curves of S is the mirror of Figure 4.) We will show that in most cases the bypass reduces n , leading to a contradiction. In particular, we have the following claim.

Claim 4.3. *If $c \cap (P'_1 \cup P'_2)$ has at most one component and $n \geq 2$, then we can destabilize \mathcal{L} (contradicting the maximality of $\text{tb}(\mathcal{L})$) except possibly when $n = 3$, in which case we can change s by 1 or -1 depending on whether c is on γ or γ' .*

Remark 4.4. In the proof below notice that when $n = 3$ we can sometimes destabilize \mathcal{L} and sometimes change s . In the exceptional case when \mathcal{L} does not destabilize notice that s must be relatively prime to n . Thus we can only attach such an exceptional bypass once and any subsequent bypasses attached from the same side of S , if it exists, cannot be exceptional and must then provide a destabilization of \mathcal{L} .

We first prove the claim, then use it to complete the proof of the lemma.

Proof of Claim. First note that if $c \cap (P'_1 \cup P'_2) = \emptyset$, then when we attach the bypass to A , we see a destabilization for \mathcal{L} in the complement of \mathcal{K} , which contradicts the maximality of $\text{tb}(\mathcal{L})$. Thus to prove the claim, we may assume that $c \cap (P'_1 \cup P'_2)$ has one component. We treat the cases $n \geq 4$, $n = 3$, and $n = 2$ separately. For $n \geq 4$, there are 8 subcases shown in Figure 21. The subcases for γ' (when the bypass is attached from the back) are the mirrors of these cases. In subcases 3, 4, 7, 8, one can use bypass rotation, Lemma 2.2, to obtain a

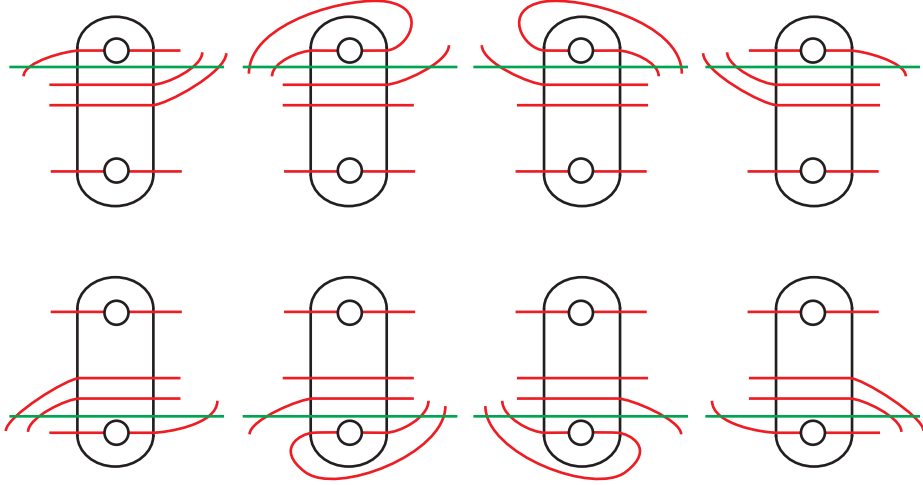


FIGURE 21. The 8 subcases of Case 2 (ordered left to right and top to bottom).

bypass disjoint from $(P'_1 \cup P'_2)$ and hence destabilize \mathcal{L} . The bypasses in subcases 2 and 6 are disallowed: if there is a bypass there then we would have a convex sphere with disconnected dividing set, contradicting tightness. In subcases 1 and 5 we can still destabilize \mathcal{L} if $n > 3$. Thus we contradict the minimality of n in all subcases except when $n \leq 3$.

For $n = 3$, we argue as above except for subcases 1 and 5. In these cases, notice that attaching the bypass does not destabilize \mathcal{L} but it does alter the dividing curves. Specifically pushing across the bypass adds (or subtracts, in the case of γ') 1 to the slope of Γ_A once we have renormalized everything after attaching the bypass. Thus we see that when $n = 3$ we can either destabilize \mathcal{L} or change the slope of s by 1. This establishes the $n = 3$ case of the claim.

Finally, for $n = 2$, there are 4 subcases analogous to Figure 21. It is readily checked, as above, that two of these are disallowed by tightness, while the other two lead to destabilizations of \mathcal{L} . \square

We now return to the proof of the lemma. Since the statement of the lemma is known for $m = 0, 1, \pm 2$ by the classification of Legendrian unknots, torus knots, and the figure eight knot [5, 8], we need only check it for $|m| > 2$. As mentioned in Remark 4.4, there is an exceptional case when $s = 3$ and the destabilization argument cannot be applied directly; we ignore this case for now and return to it at the end of the proof.

Since γ'_1 and γ'_2 are parallel, the intersection of γ' with $\Gamma_{S \setminus N}$ must be essential. It follows that $|\gamma'_i \cap \Gamma_A| = |s - nm|$ for $i = 1, 2$, since γ'_i has slope nm and Γ_A has slope s . Now if $|\gamma'_i \cap \Gamma_A| \geq 2$ for $i = 1, 2$, then for any bypass c along γ' , $c \cap (P'_1 \cup P'_2)$ has at most one component. Thus we can apply the claim if $|s - nm| \geq 2$. It is an easy exercise in algebra to check that $|s - nm| \geq 2$ for all m with $|m| > 2$ whenever $n \geq 2$ and $|s| \leq 3n - 2$. This establishes the lemma when (n, s) is in the shaded region in the left diagram of Figure 22.

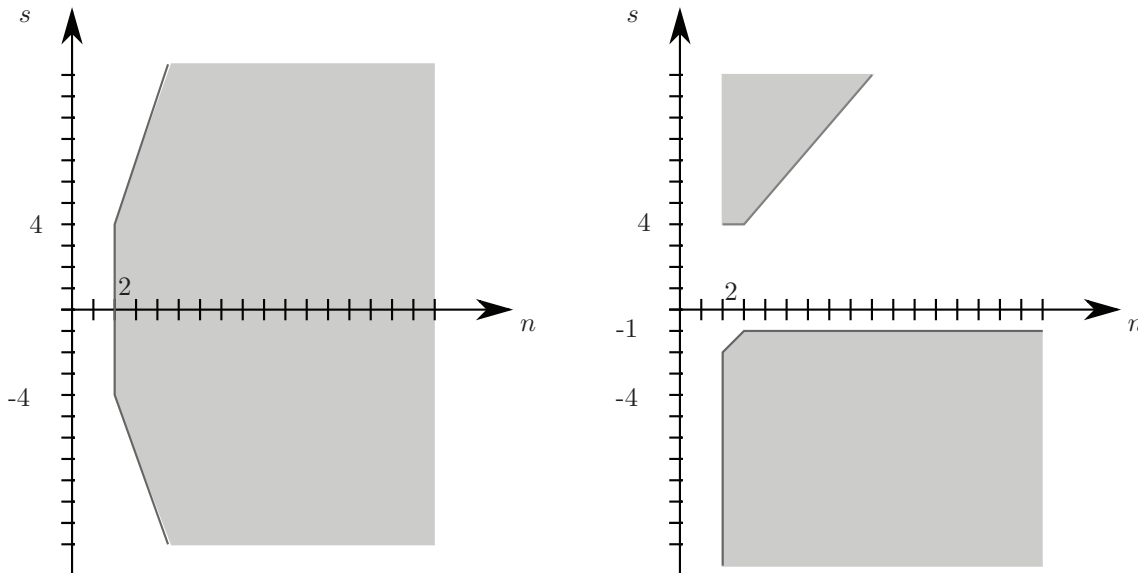


FIGURE 22. The pairs (n, s) where the destabilization of γ' gives a bypass satisfying the conditions of Claim 4.3 (left), and the pairs (n, s) where the destabilization of γ gives a bypass satisfying the conditions of Claim 4.3 (right).

Similarly, if $|\gamma_i \cap \Gamma_A| \geq 2$ for all but at most one of $i = 1, 2, 3, 4$ and $|\gamma_i \cap \Gamma_A| \geq 1$ for the other i , then we can apply the claim to at least one of the (at least two) bypasses along γ . Now the intersection of γ and $\Gamma_{S \setminus N}$ is essential if the signs of $s - 2, s, s - n, s - n + 2$ all agree. This is because in this case, a cancellation can only occur around an arc going through one of the P_i 's, and there the signs of the crossings agree with two of the above signs, so they cannot cancel. Given that the intersection of γ and $\Gamma_{S \setminus N}$ is essential, we have $|\gamma_1 \cap \Gamma_A| = |s - 2|$, $|\gamma_2 \cap \Gamma_A| = |s|$, $|\gamma_3 \cap \Gamma_A| = |s - n|$, and $|\gamma_4 \cap \Gamma_A| = |s - n + 2|$. Thus we can apply the claim and establish the lemma if the following conditions hold:

- the signs of $s - 2, s, s - n, s - n + 2$ all agree;
- at least three of $|s - 2|, |s|, |s - n|, |s - n + 2|$ are ≥ 2 , and the fourth is ≥ 1 .

The set of (n, s) for which these conditions hold is the shaded region in the right diagram of Figure 22.

The union of the shaded regions in Figure 22 covers all of the half-plane $\{(n, s) : n \geq 2\}$. This covers all possible cases, and thus if $n \neq 3$ the knot \mathcal{L} can always be destabilized by the claim, yielding the desired contradiction. When $n = 3$ notice that we can always find two

successive bypass attachments along arcs on γ or γ' that intersect $(P'_1 \cup P'_2)$ at most one time. (To see this notice that if there are not two bypasses along γ' then from above we see that $s = \pm nm, \pm(nm \pm 1)$ or $\pm(nm \pm 2)$. Given that $|nm| \geq 6$ we see that in these cases we can find the two bypasses along γ .) Thus, Remark 4.4 shows that \mathcal{L} can be destabilized in this case too. \square

Proof of Theorem 4.1. Throughout this proof we use the notation established at the beginning of this section and in the proof of Lemma 4.2. In particular notice that $P = P_1 \cup P_2 \cup A$. We also set $P' = P'_1 \cup P'_2 \cup A$, that is, P' is P with annular neighborhoods of its boundary removed (in which there can be twisting of the dividing curves).

We begin by using Lemma 4.2 to obtain a Legendrian unknot L with $\text{tb} = -1$ as described in the lemma. We then use L to create the pieces P_1, P_2, A mentioned above. We will now analyze these pieces.

Recall that we have identified A with $S^1 \times [0, 1]$ with S^1 having length 2, that is, $S^1 = [0, 2]/\sim$, where \sim identifies the endpoints of the interval. We further arrange that the dividing curves Γ_A intersect the boundary of A at $\{0, 1\} \times \{0, 1\}$. In these coordinates the slope of Γ_A is some integer. In Figure 23 we show two examples, one on the left with slope 0, and one on the right with slope 1. All other slopes can be obtained from one of these examples by applying some number of Dehn twists along a curve parallel to the boundary of A .

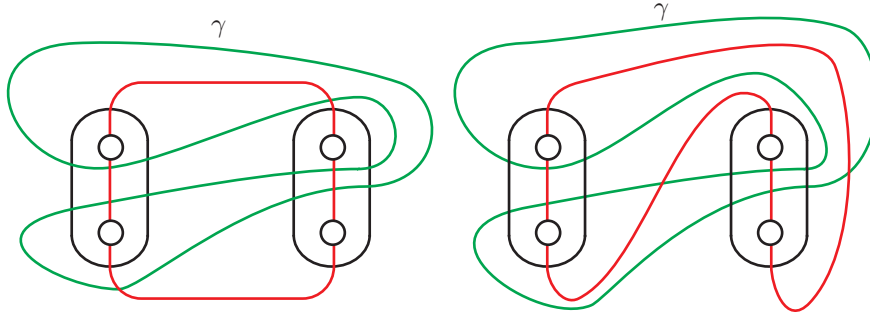


FIGURE 23. On the left the dividing curves have slope 0 on A , while on the right they have slope 1.

As in the proof of Lemma 4.2 we notice that there is always a bypass for P' on the disk D_{out} with boundary γ . Suppose the bypass is attached to P' along a curve c . There are three cases to consider: (1) c is disjoint from $P_1 \cup P_2$; (2) it has an endpoint in P_1 or P_2 ; or (3) the center intersection point of c with $\Gamma_{P'}$ is contained in P_1 or P_2 . (Notice that the last two cases do not have to be disjoint if the slope of Γ_A is near zero.) We consider further subcases depending on the slope of Γ_A , which we denote by s .

If $s > 2$, then Case (1) results in a reduction of the slope by 2, Case (2) results in a reduction of the slope by 1, and Case (3) is disallowed since it results in a disconnected dividing curve on S , contradicting the tightness of the standard contact structure on S^3 . Thus in this case, we can attach bypasses to P to arrange that $s = 2, 1$, or 0.

If $s < -1$, then Cases (1) and (2) are disallowed, and Case (3) increases the slope by 1. Thus in this case we can assume that $s = -1$.

We have now arranged that $s = 2, 1, 0$, or -1 . If $s = -1$, then there are ten possible bypass attachments. Most are disallowed, while the ones that are allowed can be used, after bypass rotation using Lemma 2.2, to increase the slope of Γ_A to 0. If $s = 0$, then there are six possible places for a bypass along γ ; see the left hand side of Figure 23. Of these, two give a disallowed bypass and the other four, after bypass rotation using Lemma 2.2, can be used to increase the slope of Γ_A to 1.

If $s = 2$, then there are ten possible bypass attachments. Of these, four reduce the slope to 1, and four are disallowed. The remaining two change the dividing curve on P to the one shown in Figure 24 with $s = 3$. Examining the eight possible bypasses in this new situation,

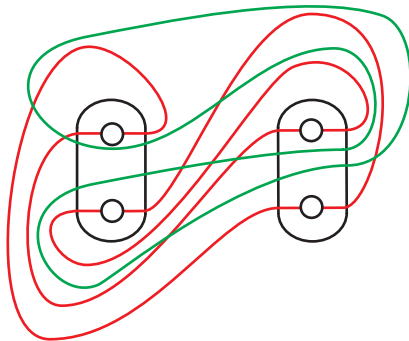


FIGURE 24. The dividing curve after bypass attachment.

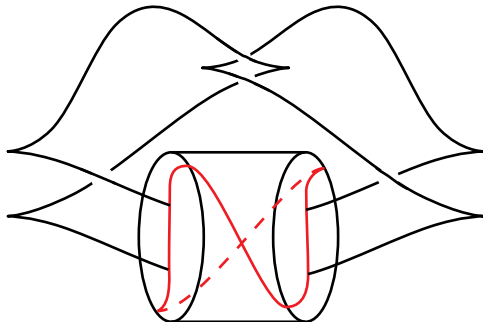
one sees that six are disallowed and the remaining two return Γ_P to the configuration with $s = 1$.

We have proved that the dividing curves on P' can be made to look like those in Figure 17. To complete the proof of the theorem, notice that we have a standard neighborhood N of \mathcal{K} as claimed and the dividing curves on P can differ from those in the figure only by twisting in the annuli $A_{i,j}$ with $i, j = 1, 2$. We can add a small neighborhood of the annuli $A_{i,j}$ to N to get a new standard neighborhood of \mathcal{K} (notice the slope of the dividing curves does not change as the neighborhood is increased to contain the annuli) and the surface P' for the old neighborhood is the surface P for the new neighborhood. This completes the proof of the theorem. \square

4.2. The contact structure in B_{out} . In this subsection we prove that either the Legendrian knot \mathcal{K} destabilizes or the Legendrian tangle in B_{out} is determined.

Theorem 4.5. *Let \mathcal{K} be a Legendrian knot in the knot type K_m , $m \neq -1$. Assume we have chosen an identification of \mathcal{K} with the standard model as in Theorem 4.1. Let $D = \{x^2 + z^2 \leq 1\} \times \{y = 0\}$ be a convex disk in $\mathbb{R}^3 \subset S^3$. Then either \mathcal{K} destabilizes or there is a contactomorphism from B_{out} to the complement of (the interior of) a standard neighborhood $\{(x, y, z) \mid x^2 + z^2 \leq 1, y^2 \leq 1\}$ of D in S^3 (with corners rounded) taking $\mathcal{K} \cap B_{\text{out}}$ to the curves shown in Figure 25.*

We notice that the dividing curves on the boundary of the ball in Figure 25 and the ones on B_{out} in Figure 17 are not the same but that there is a diffeomorphism of the ball that takes one set of curves to the other.

FIGURE 25. Model for a non-destabilizable tangle in B_{out} .

Proof. Let B be the complement of the interior of a neighborhood of D in S^3 with corners rounded and let l_1 (left) and l_2 (right) be the two Legendrian arcs in B shown in Figure 25. Let $N_1 = D^2 \times [0, 1]$ and $N_2 = D^2 \times [0, 1]$ be product neighborhoods of l_1 and l_2 , respectively. We can assume each $N_i \cap \partial B$ consists of two disks, each of which intersects the dividing curve $\Gamma_{\partial B}$ in an arc. We can further assume that the characteristic foliation of ∂B has the boundary of these disks as the union of leaves, and we can arrange that ∂N_i is convex.

Notice that $H = B \setminus (N_1 \cup N_2)$ is a genus 2 handlebody whose boundary is a surface with corners. Two disks D_1 and D_2 that cut H into a 3-ball are indicated in Figure 27. (To see where the disks come from notice that one can isotope the picture into a standardly embedded genus 2 handlebody in S^3 by isotoping the neighborhoods N_1 and N_2 so that they do not twist around each other. See Figure 26. The disks are now obvious. Isotoping back to the original

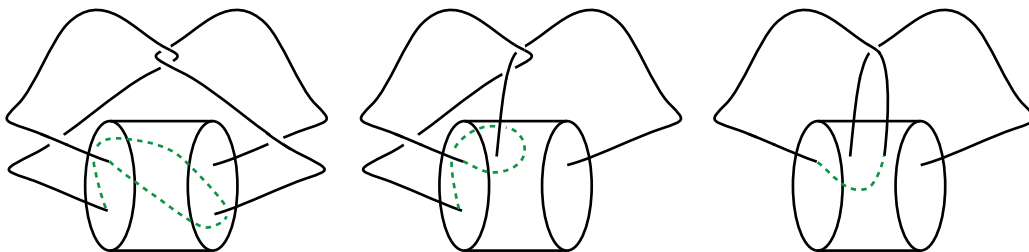


FIGURE 26. On the right hand side we see there is an obvious disk bounded by the dotted curve and one of the arcs in B . The boundary of this disk is shown in the middle and left hand pictures after the arcs in B are isotoped. On the right hand side we see the boundary of a disk that will provide a compressing disk for H .

picture, once can track the boundaries of the disk to obtain Figure 27.)

We now proceed to see what data determines the contact structure on H . A contact structure on a neighborhood N_b of ∂H is determined by the characteristic foliation on ∂H . We can find a slightly smaller handlebody \widehat{H} in H such that $\partial \widehat{H}$ is contained in N_b and is obtained by rounding the corners of ∂H . Let $\widehat{D}_i = D_i \cap \widehat{H}$, and Legendrian realize $L_i = \partial \widehat{D}_i$ on $\partial \widehat{H}$.

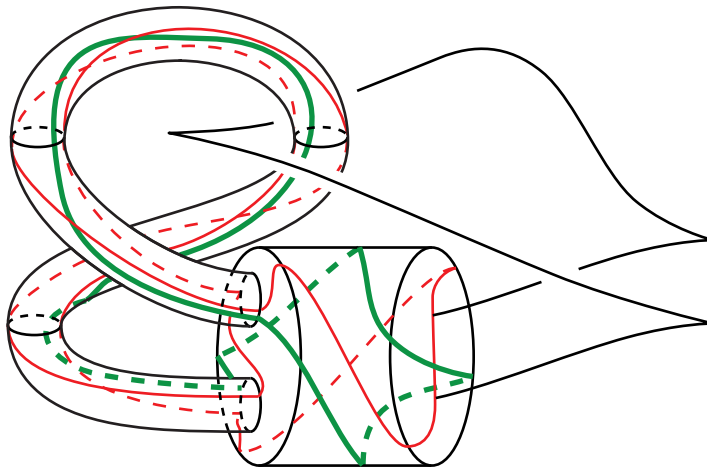


FIGURE 27. The thicker curve bounds a disk D_1 in H . The disk D_2 can be seen by reflecting this picture about a vertical line. The thinner curves depict the dividing curves.

Now L_i intersects the dividing set $\Gamma_{\widehat{H}}$ in four points, three of these points in (the part of $\partial\widehat{H}$ coming from) ∂N_i (notice that $\partial\widehat{D}_i \cap \partial N_i$ intersects the dividing set efficiently, i.e., minimally in its homology class) and one point x in (the part of $\partial\widehat{H}$ coming from) ∂B . Thus we clearly have $\text{tb}(L_i) = -2$.

Moreover, we can see that neither of the two boundary parallel dividing curves on \widehat{D}_i straddles the point x , as follows. If one did, then the other dividing curve would give a bypass attached along ∂N_i . Attaching the bypass to $\partial\widehat{H}$ will result in a surface Σ of genus two and a curve γ , which corresponds to $\partial\widehat{D}_i$ on \widehat{H} . The curve γ will intersect the dividing curves on Σ twice. Compressing Σ along a meridional disk to N_{i+1} (where we use the convention that $N_3 = N_1$) will result in a convex torus T on which γ sits. (One may also think of T as obtained by attaching the bypass to $\partial(B \setminus N_{i+1}) = \partial(H \cup N_{i+1})$.) The curve γ is an essential curve in the torus T and bounds a disk in the complement of T . Moreover, while it intersects the dividing set twice, it can be isotoped to be disjoint from it. Thus γ can be Legendrian realized, resulting in an unknot with $\text{tb} = 0$ which contradicts tightness.

The dividing set on \widehat{D}_i has now been completely determined, and so the contact structure on H is completely determined by the characteristic foliation on ∂H (and after isotoping the boundary slightly, by $\Gamma_{\partial H}$).

We now turn our attention to \mathcal{K} . We assume we have normalized \mathcal{K} , a neighborhood of \mathcal{K} , and the sphere S as in Theorem 4.1. Let l'_1 and l'_2 be the Legendrian arcs that are the components of $\mathcal{K} \cap B_{\text{out}}$ and N'_1 and N'_2 the components of $N \cap B_{\text{out}}$. The set $H' = B_{\text{out}} \setminus (N'_1 \cup N'_2)$ is a handlebody of genus 2 whose boundary is a surface with corners. We can choose disks D'_1 and D'_2 as shown in Figure 28. Notice that this figure differs from Figure 25 by a diffeomorphism of B_{out} and agrees with Figure 16 and the conclusion in Theorem 4.1. (We should take a neighborhood of $\partial H'$ and then take another copy of the handlebody with the corners on the boundary rounded as we did above, but for simplicity we will not include

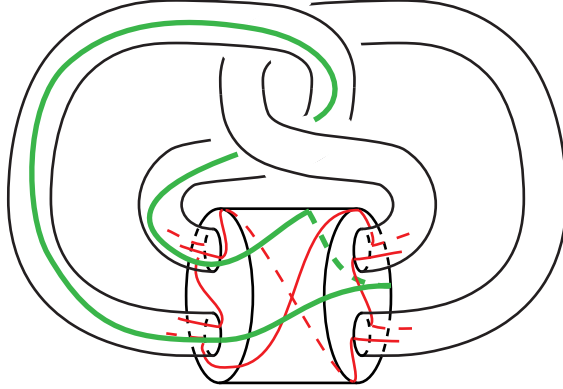


FIGURE 28. The thicker curve bounds a disk D'_1 in H' . The disk D'_2 can be seen by reflecting this picture about a vertical line.

this in the notation.) Legendrian realize $L'_i = \partial D'_i$. We see that L'_i intersects the dividing set on ∂B_{out} exactly twice, once near N'_i (and this intersection point can be assumed to be on N'_i) and once at some point y . While the intersection is efficient, as above, if we consider $\partial(B_{\text{out}} \setminus N'_i)$ then the intersection is inefficient. If $\text{tb}(L_i) \leq -3$ then there is a bypass for $\partial N_i \cap \partial H'$ along D'_i .

Notice that K_m bounds a singular disk D' with a single clasp singularity.

Claim 4.6. *The bypass above coming from D'_i can be thought of as a bypass along $\partial D'$.*

Notice that the framing given to K_m by D' is $(-1)^m$. From Proposition 2.6, the maximal Thurston–Bennequin number of K_m is ≤ 1 when m is even and ≤ -1 when m is odd; it follows that the contact framing on \mathcal{K} is always less than or equal to the framing given by D' . Thus a bypass along $\partial D'$ always gives a destabilization of \mathcal{K} .

To clarify the what the claim says, recall that the effect of attaching a bypass to a convex surface is entirely determined by its arc of attachment. Thus as long as the arc of attachment for a bypass on D'_i is a subset of $\partial D'$ then we may assume it is a bypass on D' as far as its effect on ∂N is concerned.

Proof of Claim. Notice that $\partial D'$ can be broken into two parts $c_1 = \partial D' \cap N_i$ and $c_2 = (\partial D') \setminus c_1$. Moreover we can assume that $c_1 = \partial D'_i \cap N_i$. If c_1 intersects the dividing curves on ∂N_i efficiently then with the appropriate orientations on c_1 and the dividing curves, all the intersections between c_1 and the dividing curves are negative, since if not then we could add a neighborhood of a Legendrian arc in B_{in} to N_i to construct a neighborhood of a Legendrian unknot with nonnegative Thurston–Bennequin number, contradicting tightness. We can similarly assume c_2 negatively intersects the dividing curves on $N \setminus N_i$, where the orientation on the dividing curves and c_2 are consistent with the orientations chosen for the dividing curves on N_i and c_1 . We have shown that we can arrange that $\partial D'$ intersects the dividing curves on ∂N efficiently and $\partial D' \cap N_i = \partial D'_i \cap N_i$. Hence any bypass along $\partial D'_i$ for ∂N_i can be thought to be a bypass attached along $\partial D'$. \square

We assume for the remainder of this proof that \mathcal{K} does not destabilize. It follows from the above discussion that $\text{tb}(L'_i) = -2$ or -1 . Arguing as we did for the standard model above, we see that $\text{tb}(L'_i)$ cannot equal -1 , so we may assume $\text{tb}(L'_i) = -2$. Moreover, as above, we see that neither of the two boundary parallel dividing curves on D'_i can straddle y . Thus the configuration of the dividing curves $\Gamma_{D'_i}$ is determined, and the contact structure on H' is determined by the characteristic foliation on $\partial H'$.

We can thus find a diffeomorphism $\phi : B \rightarrow B_{\text{out}}$ that preserves the dividing set on the boundary and takes l_i to l'_i and D_i to D'_i . Since ϕ can be isotoped to be a contactomorphism in a neighborhood of $(\partial B) \cup l_1 \cup l_2$ and the dividing curves on D_i and D'_i are determined above, we can isotope ϕ to be a contactomorphism from B to B_{out} taking $l_1 \cup l_2$ to $l'_1 \cup l'_2 = \mathcal{K} \cap B_{\text{out}}$. \square

4.3. The contact structure in B_{in} and braids. The disc $D = \{x^2 + z^2 \leq 1\} \times \{y_0\}$ is convex in (S^3, ξ_{st}) with dividing curve $\Gamma_D = \{0\} \times [-1, 1] \times \{y_0\}$. Fix m points $\{(-1 + \frac{2i}{m+1}, y_0, 0)\}_{i=1}^m$ on Γ_D . Then the fronts of Legendrian braids in $D \times [-1, 1]$ with endpoints $\{(-1 + \frac{2i}{m+1}, -1, 0)\}_{i=1}^m \cup \{(-1 + \frac{2i}{m+1}, 1, 0)\}_{i=1}^m$ are described as follows:

Theorem 4.7 (Etnyre and Vértesi[12]). *The Legendrian representations of a braid in $D \times [-1, 1]$ are built up from the building blocks of Figure 29.* \square

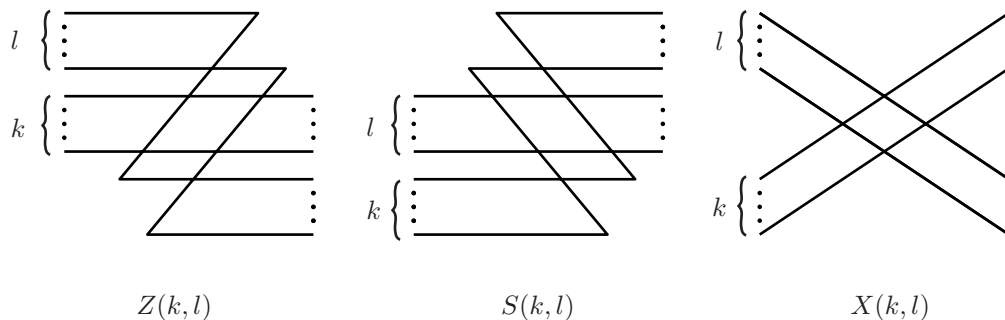


FIGURE 29. Building blocks of Legendrian braids. There can be other horizontal strands, not depicted, above and/or below the strands shown..

Note that $Z(0, 1)$ and $S(1, 0)$ are just stabilizations. Using Theorem 4.7 we can understand Legendrian braids with two strands; we will write $Z = Z(1, 1)$, $X = X(1, 1)$, $S = S(1, 1)$. Notice that if Z or S is followed by X or vice versa then it destabilizes, see Figure 30. This observation immediately yields the following result.

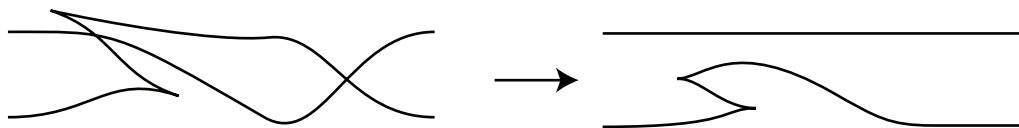


FIGURE 30. $S = S(1, 1)$ followed by $X = X(1, 1)$ is Legendrian isotopic to a trivial braid with one stabilization.

Proposition 4.8. *Consider a braid with two strands and n half twists.*

- (1) *If $n \geq 0$ then a Legendrian representation of B either destabilizes or consists of n blocks of type X ;*
- (2) *If $n < 0$ then a Legendrian representation of B either destabilizes or is built up from n building blocks of type S and Z in any order. \square*

This proposition allows us to understand $\mathcal{K} \cap B_{\text{in}}$.

Theorem 4.9. *Let \mathcal{K} be a Legendrian knot in the knot types $K_m, m \neq -1$. Either \mathcal{K} destabilizes or the contactomorphism from B_{out} to a ball in S^3 given in Theorem 4.5 can be extended to B_{in} , giving a contactomorphism from S^3 to itself that maps $\mathcal{K} \cap B_{\text{in}}$ to a Legendrian braid on two strands with $m + 2$ twists.*

Proof. The contactomorphism clearly extends as a diffeomorphism and since there is a unique contact structure up to isotopy on the 3-ball, we can isotope this diffeomorphism (relative to B_{out}) to a contactomorphism on B_{in} . The image of $\mathcal{K} \cap B_{\text{in}}$ is clearly a Legendrian 2-braid with $m + 2$ twists. \square

We are now ready to simultaneously prove Theorems 3.1, 3.2, and 3.3.

Proof of Theorems 3.1, 3.2, and 3.3. If $m \neq -1$, let \mathcal{K} be a Legendrian realization of K_m . From the previous theorem either \mathcal{K} destabilizes or there is a contactomorphism of S^3 taking \mathcal{K} to one of the Legendrian knots shown on the left of Figure 9; note that the box shown there is a Legendrian 2-braid. If there is not an obvious destabilization of the 2-braid, then by Proposition 4.8, it is obtained by stacking $|m + 2|$ S 's and Z 's together if $m \leq -2$, or $m + 2$ X 's if $m \geq 0$. Clearly this agrees with Figure 9 for $m \leq -2$, but also notice that for $m \geq 0$ this gives a knot isotopic to the one in Figure 10. Since Legendrian isotopy in the standard contact structure on S^3 is the same as ambient contactomorphism (i.e., a contactomorphism sending one Legendrian knot to the other) [3], this completes the proof once we know that the knots shown in Figures 9 and 10 do not destabilize. But this is the content of Proposition 2.6. \square

REFERENCES

- [1] Joan S. Birman and William W. Menasco. Stabilization in the braid groups. II. Transversal simplicity of knots. *Geom. Topol.*, 10:1425–1452 (electronic), 2006.
- [2] Yuri Chekanov. Differential algebra of Legendrian links. *Invent. Math.*, 150(3):441–483, 2002.
- [3] Yakov Eliashberg. Legendrian and transversal knots in tight contact 3-manifolds. In *Topological methods in modern mathematics (Stony Brook, NY, 1991)*, pages 171–193, 1993.
- [4] Yakov Eliashberg. Invariants in contact topology. In *Proceedings of the International Congress of Mathematicians, Vol. II (Berlin, 1998)*, number Extra Vol. II, pages 327–338 (electronic), 1998.
- [5] Yakov Eliashberg and Maia Fraser. Classification of topologically trivial Legendrian knots. In *Geometry, topology, and dynamics (Montreal, PQ, 1995)*, pages 17–51, CRM Proc. Lecture Notes, 15, 1998.
- [6] Judith Epstein, Dmitry Fuchs, and Maike Meyer. Chekanov-Eliashberg invariants and transverse approximations of Legendrian knots. *Pacific J. Math.*, 201(1):89–106, 2001.
- [7] John B. Etnyre. Legendrian and transversal knots. In *Handbook of knot theory*, pages 105–185. Elsevier B. V., Amsterdam, 2005.
- [8] John B. Etnyre and Ko Honda. Knots and contact geometry. I. Torus knots and the figure eight knot. *J. Symplectic Geom.*, 1(1):63–120, 2001.
- [9] John B. Etnyre and Ko Honda. On connected sums and Legendrian knots. *Adv. Math.*, 179(1):59–74, 2003.

- [10] John B. Etnyre and Ko Honda. Cabling and transverse simplicity. *Ann. of Math. (2)*, 162(3):1305–1333, 2005.
- [11] John B. Etnyre, Douglas J. LaFountain, and Bülent Tosun. Legendrian and transverse cables of positive torus knots. arXiv:1104.0550, 2011.
- [12] John B. Etnyre and Vera Vértesi. Satellites and positive braids. In preparation, 2011.
- [13] Dmitry Fuchs. Chekanov–Eliashberg invariant of Legendrian knots: existence of augmentations. *J. Geom. Phys.*, 47(1):43–65, 2003.
- [14] Emmanuel Giroux. Convexité en topologie de contact. *Comment. Math. Helv.*, 66(4):637–677, 1991.
- [15] Ko Honda. On the classification of tight contact structures. I. *Geom. Topol.*, 4:309–368 (electronic), 2000.
- [16] Ko Honda, William H. Kazez, and Gordana Matić. Right-veering diffeomorphisms of compact surfaces with boundary. *Invent. Math.*, 169(2):427–449, 2007.
- [17] Yutaka Kanda. The classification of tight contact structures on the 3-torus. *Comm. Anal. Geom.*, 5: 413–438, 1997.
- [18] Paolo Lisca, Peter Ozsváth, Andras Stipsicz, and Zoltan Szabó. Heegaard Floer invariants of Legendrian knots in contact three-manifolds. *J. Eur. Math. Soc. (JEMS)*, 11(6):1307–1363, 2009.
- [19] Lenhard L. Ng. Maximal Thurston–Bennequin number of two-bridge links. *Algebr. Geom. Topol.*, 1:427–434, 2001.
- [20] Lenhard Ng and Lisa Traynor. Legendrian solid-torus links. *J. Symplectic Geom.*, 2(3):411–443, 2004.
- [21] Peter Ozsváth and Andras Stipsicz. Contact surgeries and the transverse invariant in knot Floer homology. *J. Inst. Math. Jussieu*, 9(3):601–632, 2010.
- [22] P. E. Pushkar’ and Yu. V. Chekanov. Combinatorics of fronts of Legendrian links, and Arnol’d’s 4-conjectures. *Uspekhi Mat. Nauk*, 60(1(361)):99–154, 2005.
- [23] Dan Rutherford. The Thurston–Bennequin number, Kauffman polynomial, and ruling invariants of a Legendrian link: the Fuchs conjecture and beyond. *Int. Math. Res. Not.*, vol. 2006, Art. ID 78591, 1–15, 2006.
- [24] Joshua M. Sabloff. Augmentations and rulings of Legendrian knots. *Int. Math. Res. Not.*, (19):1157–1180, 2005.

SCHOOL OF MATHEMATICS, GEORGIA INSTITUTE OF TECHNOLOGY, 686 CHERRY ST., ATLANTA, GA 30332
E-mail address: etnyre@math.gatech.edu
URL: <http://math.gatech.edu/~etnyre>

MATHEMATICS DEPARTMENT, DUKE UNIVERSITY, DURHAM, NC 27708
E-mail address: ng@math.duke.edu
URL: <http://www.math.duke.edu/~ng>

DEPARTMENT OF MATHEMATICS, MASSACHUSETTS INSTITUTE OF TECHNOLOGY, 77 MASSACHUSETTS AVENUE, CAMBRIDGE, MA 02139
E-mail address: vertesi@math.mit.edu